

The role of d-orbital polarization on rhodium cluster collisions*

F. Muñoz^{1,2}, J. Rogan^{1,2}, G. García^{2,3}, J.A. Valdivia^{1,2}, R. Ramírez^{2,3}, and M. Kiwi^{1,2,3,a}

¹ Departamento de Física, Facultad de Ciencias, Universidad de Chile, Casilla 653, Santiago, Chile

² Centro para el Desarrollo de la Nanociencia y la Nanotecnología, CEDENNA, Avda. Ecuador 3493, Santiago, Chile

³ Facultad de Física, Pontificia Universidad Católica de Chile, Casilla 306, 7820436 Santiago, Chile

Received 20 January 2011 / Received in final form 8 April 2011

Published online 29 July 2011 – © EDP Sciences, Società Italiana di Fisica, Springer-Verlag 2011

Abstract. The effects due to *d*-orbital polarization in collision processes between a single rhodium atom and a 12 atom rhodium cluster are investigated by means of ab initio molecular dynamics. For the initial configuration of the 12 atom rhodium targets we adopt two different low energy structures. The kinetic energy and impact parameter of the projectile are chosen in such a way that fusion, scattering and fragmentation of the cluster do occur. The collision is treated by means of density functional theory molecular dynamics (DFT-MD). Both spin unpolarized and polarized treatments are implemented in order to clearly distinguish the effects that are due to *d*-orbital polarization. We find a novel block dynamics, of parts of the cluster, which is due to the directional nature of *d*-bonds. In addition, the treatment of the collisions by means of high temperature DFT dynamics yields promising minimal energy configurations, which are target dependent but are difficult to obtain otherwise.

1 Introduction

The description of nanocluster collisions has attracted considerable interest for some time. From a theoretical point of view the status of the field received significant impetus with the increased availability of modern computers, which led to a wealth of significant results, already reviewed in detail by Andersen et al. [1–3] more than a decade ago. Certainly, the last decade has seen a considerable addition of new information to the field. Initially the problem was treated using classical molecular dynamics (MD) but more recently, with the considerable increase in computer capability, quantum mechanical approaches have become feasible, at least for the collision of small clusters. In 2000 Chien et al. [4], using simple binary potentials, investigated the geometric configuration of Rh clusters of up to 58 atoms. Rogan et al. [5] investigated using classical MD the collision of small gold clusters, for a wide range of energy and impact parameter values. Later on MD calculations, using embedded atom type potentials, were implemented to obtain the configurations and treat the collisions of metallic clusters of hundreds of atoms.

On the other hand, reliable results can only be obtained by means of a quantum mechanical treatment, that is by using ab initio techniques. Recently, Muñoz et al. [6] used a DFT formalism to investigate the collision between a single Au atom and a Au₁₃ target cluster, and found important differences with the semi-classical treatment by Rogan et al. [5]. For instance, the relevant fragmentation energies obtained with DFT were found to be a full order of magnitude larger than those obtained by means of a semi-classical treatment, mainly due to the rearrangement of the electron cloud.

But gold is somewhat special, due to its full *d*-shell. Therefore, the bonding is dominated by *s*-electrons and the spin-polarization effects – if any – are minimal and play no role in the collision dynamics. However, the effects due to incomplete *d*-shells on both bonding and spin-polarization are relevant features for metal clusters. In this context rhodium clusters seem to be perfect candidates to extend our understanding and to contrast with results on gold clusters [6]. It is well known that they develop a magnetic moment [7,8] for sizes up to ∼60 atoms, while larger clusters and bulk Rh are non-magnetic. This behavior has attracted the attention of basic and applied researchers, because of the implications it has for the magnetic recording industry [9]. In fact, while the structural characterization – and hence the magnetism – of Rh clusters is an open problem, they have potential for use as a high density storage media, and also find applications in catalysis, as pointed out by Wei and Iglesia [10] and by Nolte et al. [11]. Another characteristic of Rh is its large bulk

* Supported by the *Fondo Nacional de Investigaciones Científicas y Tecnológicas* (FONDECYT, Chile) under grants 1090225 (MK and JR), 1080239 (GG and RR), 1070854 and 1110135 (JAV), and *Financiamiento Basal para Centros Científicos y Tecnológicos de Excelencia*.

a e-mail: mkiwi@puc.cl

melting and evaporation temperatures, which are ~ 900 K larger than for Au. Certainly, the strong Rh bonds also play a major role in the collision dynamics, but we cannot expect a mere shift (towards higher energies) relative to the gold cluster behavior, since during the early stages of the collision process the energy is well localized, and later spreads inducing a coordinated motion of all the ions of the cluster. Therefore we expect the interplay of strength, directionality, and range of the electron cloud to give rise to new phenomena.

Another interesting feature of Rh clusters of up to ~ 27 atoms is their predicted simple cubic structure [12,13]. Actually for Rh_{13} the cubic geometry is significantly more favorable, by ~ 1 eV, as compared with more compact icosahedral conformations [14–16]. This behavior has been conjectured to be related to the tendency of d -orbitals to form eight-center bonds at right angles [12] and moreover, these cubic geometries were predicted to have a smaller magnetic moment than the more compact ones, a feature that is consistent with experimental data [7,8]. Strangely, the lower magnetic moment of the less coordinated cubic structure is the opposite of the usual behavior of magnetic metals like Co [17], which has the same number of valence electrons, i.e. it lies just one row further up in the periodic table.

Within a collision context, the strong – and strongly directional – bonding of Rh, can yield a radically different collision dynamics from the one obtained for Au. The naive picture is to assume that the main difference with the Au case should be just a larger likelihood of fusion with the target. However, the directional and short-ranged nature of the bonds does yield a much richer behavior.

In this paper our main objective is to try to understand the role d -orbital polarization plays in the collision process and to extend the work on gold clusters [5,6] to a system with a magnetic ground state and d -bonding. An additional goal is to investigate and validate the feasibility of using collision dynamics as a method to generate a diverse bank of low energy configuration clusters, since a virtue of the procedure we put forward here is that it opens the possibility to use the collision dynamics to generate ground state structures for Au_{12} , Au_{13} and Au_{14} . Although the collision dynamics occasionally does resemble a high-temperature MD, followed by annealing, at the DFT level the outcome of both procedures is rather different. While high temperature MD has been found to have difficulties in generating highly symmetric configurations [14], our DFT collision dynamics was capable of yielding a rich diversity of configurations, both of high and low symmetry.

This paper is organized as follows: after this introduction we present the methods we use and provide the technical details of the DFT procedure in Section 2. The energy and impact parameter dependence of the results is analyzed in Section 3, while the influence of the spin dynamics is discussed in Section 4. Finally, Section 5 closes this paper with a summary and a discussion of the main results.

2 Method and computational details

The rhodium cluster collisions were simulated using the DFT formalism [18,19] as implemented in the VASP code [20–22]. In order to avoid self-interactions, or even worse, spurious interactions between fragments scattered after the collision, we use the largest possible simulation cell compatible with our computational resources (i.e. a cube of sides of ≈ 18 Å). In addition, we treat the fragments separately when they are sufficiently far apart for their interaction to be negligible. PAW pseudopotentials [23] and PBE [24–26] for the exchange-correlation were used. The energy cutoff was set to 230 eV. The targets we choose are Rh_{12} clusters that have been extensively studied at the DFT level [12–16,27–33], for which we make sure that our initial set of parameters yields an adequate description.

The calculations to obtain the groundstate structure were carried out without constraining the magnetic moment, both of the target and the projectile, and their initial magnetic moments were aligned parallel to each other. Since, unless explicitly stated, we perform the calculations implementing an unconstrained spin approach, the initial relative orientation of the magnetic moments does not play a relevant role, because the system always converges to the minimum energy state. On the other hand, if the spin is kept fixed the relative initial orientation is important, since in doing so we are forcing the system into a configuration that corresponds to an excited state. It is worth mentioning that, following the usual practice in the calculation of the electronic properties of clusters, we limit ourselves to the Γ -point in reciprocal space, which implies an integer value for the magnetic moment (i.e. the number of majority minus minority spin electrons). When spin polarization is ignored the outcome, as far as geometrical structure is concerned, changes only slightly while the energy, and especially the magnetization, are at times quite different when compared to the spin polarized calculations.

In order to carry out the simulation properly, the first step is to select a physically realistic collision target configuration, that is a low energy one. Fortunately this subject has been widely investigated and there is a general agreement [12,15,16,27,29,31,32] that the lowest energy Rh_{12} configuration is the magic number double cube structure illustrated in Figure 1, which we identify as target structure Rh^A . Also, it is of interest to compare the results of our procedure with those obtained for collisions with a more compact structure, such as the second one seen in Figure 1, since the more coordinated Rh clusters have a different kind of bonding and a larger magnetic moment. This also allows us to rule-out target specific features in our conclusions. We named this second target Rh^B , and it has an energy ≈ 2 eV larger than that of Rh^A . In addition to ruling-out target specific features, this second Rh^B target will allow us to discuss some of the magnetic interaction effects on the dynamics, as described in detail below. First we choose a proper collision target, by adopting a 12 atom Rh cluster in a minimum energy configuration, with its center of mass positioned at the origin

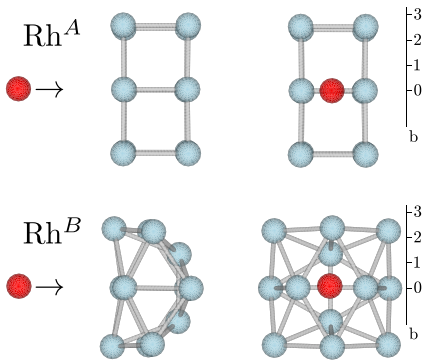


Fig. 1. (Color online) The two targets we investigate, namely Rh^A and Rh^B , are illustrated in the upper and lower panels, with lateral and frontal views given at the left and right, respectively. The targets are colored gray and the projectile red. The various impact parameters (b values), measured relative to the center of mass in Å units, are illustrated on the right.

of the simulation box. The projectile is located some distance away from the cluster and impinges orthogonally on the Rh_{12} target, as illustrated in Figure 1.

Throughout this paper the impact parameter b is given in Å units, relative to the cluster center of mass, and the initial kinetic energy E_k in eV. The target has no initial center of mass velocity and no vibrational energy (i.e. $T = 0$ K). Next, a rhodium atom is placed at ≈ 4 Å from the nearest target atom. Although this distance is relatively small, we checked that we can safely ignore the charge transfer between target and projectile before the collision process starts.

The projectile carries a kinetic energy E_k and flies toward the target with an initial impact parameter b . The simulation is carried out during 2 ps in the microcanonical ensemble, and hence the system initially evolves freely during this time, just constrained by energy conservation. After the collision takes place, and depending on the values of both E_k and b , one of following three scenarios is observed: fusion of target and projectile, target fragmentation, or projectile scattering. We define as fusion the permanent trapping of the projectile after the collision. Fragmentation corresponds to breaking up the target to yield a cluster with either 12 or less atoms, since the possibility of having the projectile captured and another atom expelled cannot be overlooked. Finally, scattering implies that after the collision the target continues to be a 12 atom cluster after the projectile is deflected. It may be worth mentioning that at least another possibility does exist, namely evaporation, but the simulation times involved in this physical process are beyond the scope of our computational resources.

Certainly, after the collision takes place the target is left in an excited (high temperature) state and to systematize our analysis of the data it is necessary to get rid of this excess excitation energy. Thus, we simulate a radiation process, or cooling down of the system after the collision, by linearly rescaling the atomic velocities until they reach room temperature, which takes an additional 3 ps of simulation time. At 300 K only the vibrational

modes of the cluster are excited, since the atoms vibrate around their equilibrium positions and the cluster structures remain invariant.

3 Energy and impact parameter dependence

The dependence of the results of the above process, on the impact parameter b and the kinetic energy E_k of the projectile, are illustrated in Figure 2 for the Rh^A , and in Figure 3 for the Rh^B targets. As mentioned above we limit our interest to three scenarios: fusion, scattering and fragmentation. Other outcomes are certainly possible, but for the time being we just consider these three regimes which are the most likely ones.

It is apparent that when the projectile impinges on the Rh^A configuration, within the parameter space we investigated, fusion is the dominant collision outcome and it occurs for almost all combinations of b and E_k values. This is in sharp contrast with the results we obtained for the closed *d*-shell metal Au [6], where the fragmentation of the cluster in the same range of E_k values strongly depends on the impact parameter b . In other words the outcome depends on the electronic density distribution of the target. Also, scattering of the projectile occurs for large b and E_k values, just as is the case with Au collisions.

A similar trend governs the Rh^B fragmentation, when compared with Au fragmentation, since it is observed only for quite large energies. But, in contrast to Au, for Rh no scattering ever occurs regardless of the b value, as can be seen in Figure 3.

The fragmentation and scattering of Rh clusters is almost instantaneous, i.e. the expelled atom is the one which receives the main impact and the fragment departs from the main cluster right after the collision. In contrast, the Au fragmentation and scattering processes occur accompanied by a significant atomic rearrangement.

The consequences of carrying out the calculations allowing for spin polarization of Rh^A are quite apparent and, at first glance, somewhat counter-intuitive. In fact, the ground state of Rh nanoparticles, including Rh_{13} , is ferromagnetic [16]. Consequently, if spin polarization is neglected one would expect a weaker binding among the target atoms (favoring fragmentation). However, precisely the opposite behavior is observed: when the spin polarization is turned off no fragmentation does occur. Nevertheless, the absence of fragmentation can be understood in terms of the internal cluster dynamics after impact, since the absence of spin polarization allows for faster and more flexible atomic rearrangements, due to weaker bonds, thus allowing the expelled atom to be recaptured, as illustrated in Figure 4.

In contrast, the inclusion of spin-polarization in the dynamics of Rh^B is less conspicuous. The only significant change is the absence of fragmentation for $b = 2$ and $E_k = 10$, when spin-polarization is ignored. The explanation for this different collision outcome has its roots in the lower momentum transferred by the projectile to the cluster atom that receives the major impact. The projectile is

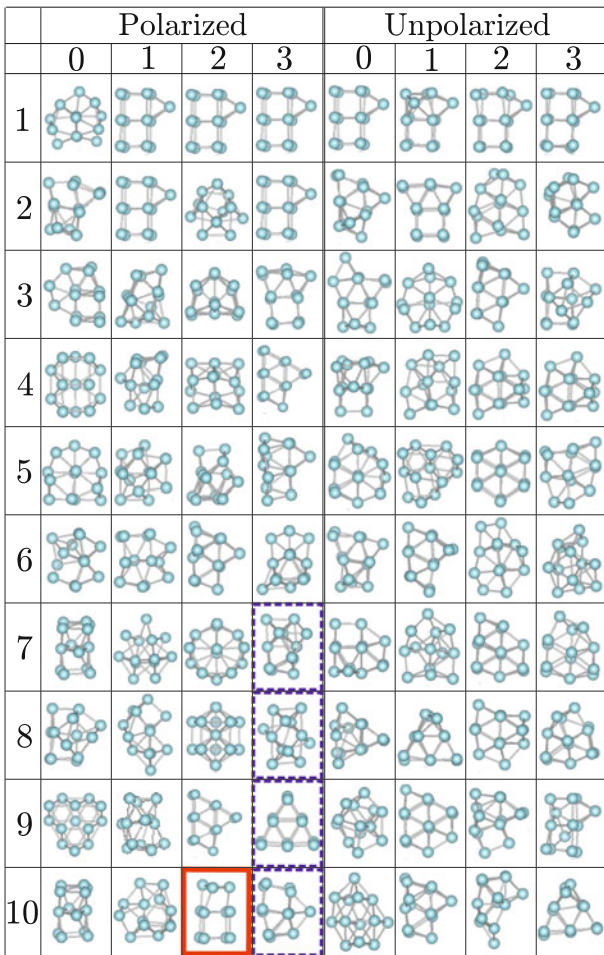


Fig. 2. (Color online) Configurations after the collision of a Rh^A cluster with a Rh atom, after the cluster has been cooled by radiation to 300 K. On the left (right) columns are the results including (ignoring) spin-polarization. The impact parameter b , measured relative to the center of mass of the target, is given in Å units and indicated at the top of the columns. The kinetic energy of the projectile E_k is at the left, in eV units. The red (continuous) and blue (dashed) frames denote fragmentation and scattering, respectively. Otherwise the outcome is fusion. In the only fragmentation case two atoms are expelled.

less attracted by the target in a spin unpolarized approximation, since it gains less kinetic energy (additional to its original E_k), and therefore transfers less energy to the cluster, thus eluding fragmentation. This explanation does not hold for the Rh^A conformation, since the extra projectile energy due to spin-polarization effects just amounts to ≈ 0.4 eV, that is, an order of magnitude smaller. The value of ≈ 0.4 eV is estimated from the potential energy vs. time plot displayed in Figure 5, where we observe that the minimum V value (at less than 100 fs) of the spin polarized plot lies ≈ 0.4 eV lower than the unpolarized one.

In Figure 6 we plot the average temperature during the collision process (that is, during the first 2 ps) before the cooling down is started. The time averaged temperature

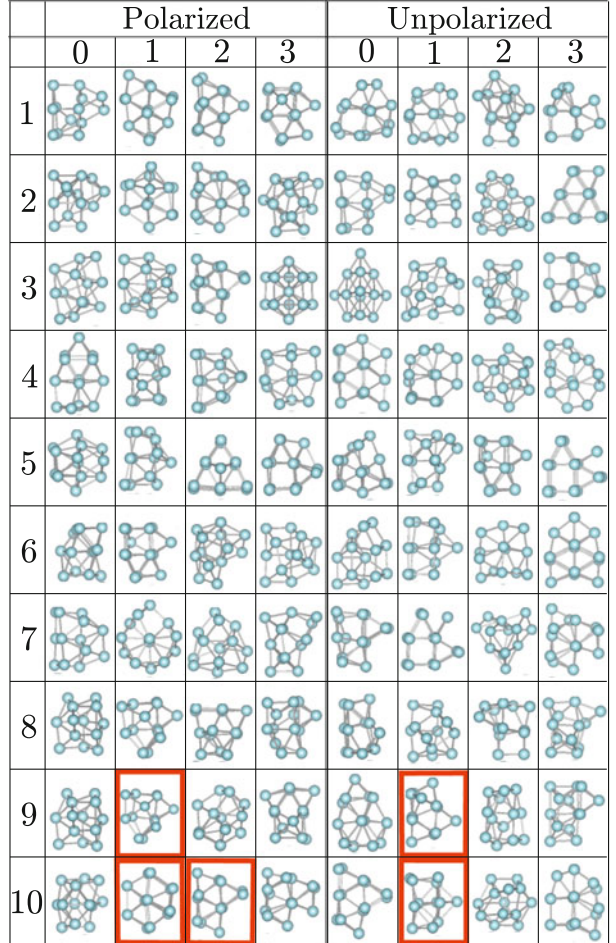


Fig. 3. (Color online) Configurations after the collision of a Rh^B cluster with a Rh atom, after the cluster has been cooled by radiation to 300 K. On the left (right) columns are the results including (ignoring) spin-polarization. The impact parameter b , measured relative to the center of mass of the target, is given in Å units and indicated at the top of the columns. The kinetic energy of the projectile E_k is at the left, in eV units. The red (continuous) and blue (dashed) frames denote fragmentation and scattering, respectively. Otherwise the outcome is fusion.

is calculated as $\langle T \rangle = \sum_{t=0}^{2 \text{ ps}} T(t)$, where we average over a $t = 1$ fs MD time step. It is interesting to notice that $\langle T \rangle$ turns out to be an approximately linear function of E_k , both for Rh^A and Rh^B , however, the deviations from linear behavior are larger for Rh^A , except for the $b = 0$ case. Actually, the time evolution of the Rh^B target, as obtained by examination of the collision movies, shows that the impact rapidly deforms the target structure, giving rise to an amorphous cluster that oscillates until the cooling down generates a low symmetry Rh_{13} configuration. This is also the case for the $b = 0$ impact on Rh^A , and is confirmed by inspection of Figures 2 and 3.

For Rh^A the departure from linearity, seen in Figure 6 for $b \neq 0$, is due to an interesting phenomenon: the impact generates major blocks (or sub-clusters) of atoms, which evolve quasi independently in the intra- and inter-block rearrangement dynamics. To illustrate this issue we

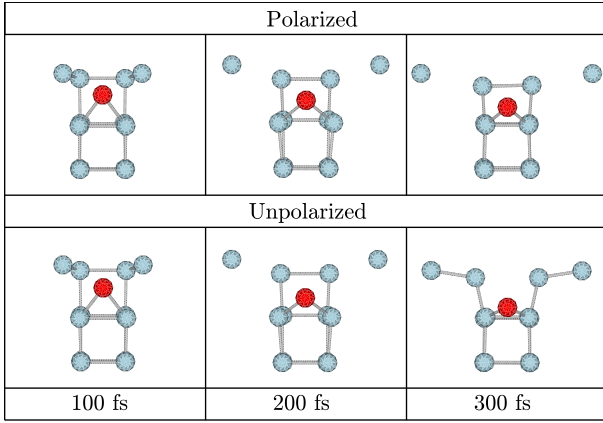


Fig. 4. (Color online) Illustration of the effect of spin polarization on the collision dynamics of a Rh atom (red) impinging on a Rh^A target, for $b = 2 \text{ \AA}$ and $E_k = 10 \text{ eV}$. The upper (lower) panel shows the time evolution including (ignoring) spin-polarization of the charge density. During the early stages (after 100 and 200 fs) the dynamics is quite similar, but when the impacted atoms “try” to escape (300 fs) the effects of spin-polarization become evident, since the main cluster is not able to recapture the fragments.

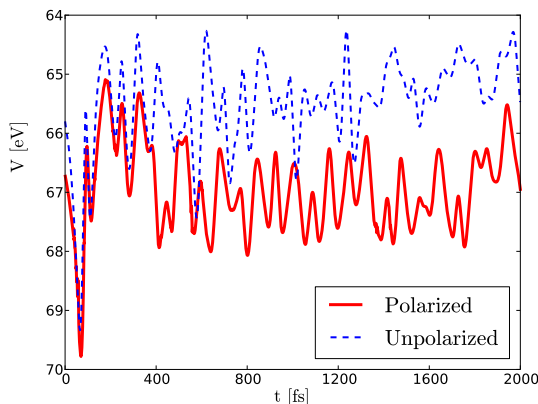


Fig. 5. (Color online) Time evolution of the potential energy V for a collision of a Rh atom with a Rh^A target, for $b = 1$ and $E_k = 3$. During the first 400 fs the dynamics is projectile-driven. At ≈ 400 fs a bifurcation occurs and spin-polarization effects lead to different atomic rearrangements.

examine the collision at 100, 200 and 300 fs, for $b = 2$ and $E_k = 10$, as displayed in the upper panel of Figure 4.

We can separate the cluster into four “building blocks” of atoms: (i) the lower Rh₄ cube, which remains mainly static; (ii) the projectile, which retains some kinetic energy after the impact and oscillates around the lower cube; (iii) the top Rh dimer, whose movement can be described as coupled to the lower cube by a hinge; and finally, (vi) the two expelled atoms. After some time, which depends on the initial parameters, the blocks can either split, merge or change shape. In this way the building blocks gradually start to lose their original high symmetry, often evolving into low symmetry compact structures, like many of the ones seen in Figure 2. However, there are

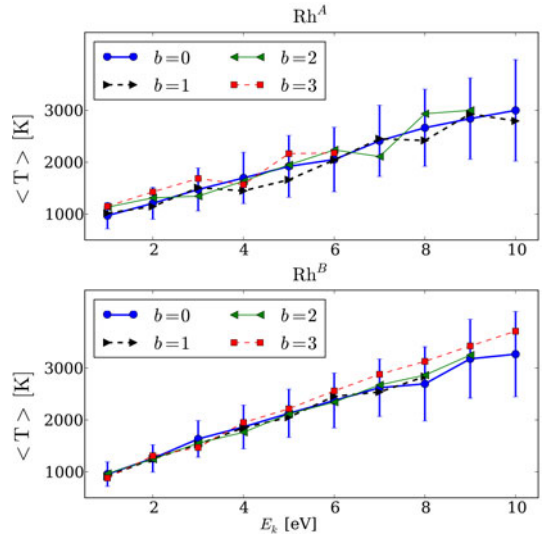


Fig. 6. (Color online) Average temperature of the 13 atom system, of projectile plus Rh^A (upper panel) and Rh^B (lower panel) targets. The error-bars denote the standard deviation, and are included solely for $b = 0$, since they are similar for all the other b values. Only spin-polarized collisions leading to fusion of target and projectile are illustrated.

cases like polarized $b = 2$ and $E_k = 10$, or low energy values and $b \neq 0$, where the dynamics of the blocks, within the collision time, partially preserves the above described building block structure.

The Rh₁₃ conformations that are created in this way are of special interest, since they are strong candidates for minimal energy configurations. In fact, in Figure 2 we do recognize the Rh₁₃ ground state [12–14], which we obtain for the polarized $\{b = 1, 2, 3; E_k = 1\}$, $\{b = 1, 3; E_k = 2\}$, and also for the unpolarized $\{b = 0, 3; E_k = 1\}$ case, in Å and eV units, respectively. Moreover, we also recognize other low-energy isomers often found in the literature [12,13,27,29,33].

4 Spin polarization

Other issues that deserve attention are (i) the cluster magnetic moment magnitude and distribution; and (ii) the relation between the time evolution and the magnetic polarization of the system. The way these issues are addressed implies conceptual choices that deserve some discussion. If the projectile and cluster are assumed to constitute a completely isolated system, then the total angular momentum \mathbf{J} should be a conserved quantity. However, our treatment is not compatible with the idea of an isolated system, since in the cooling down process heat radiation is emitted. In addition, we also assume that the angular momentum gained or lost by the system, when seeking the minimum energy configuration, is absorbed by an external reservoir. Consequently, in our treatment the energy and the angular momentum of the projectile plus target are not conserved quantities, since we do not model the

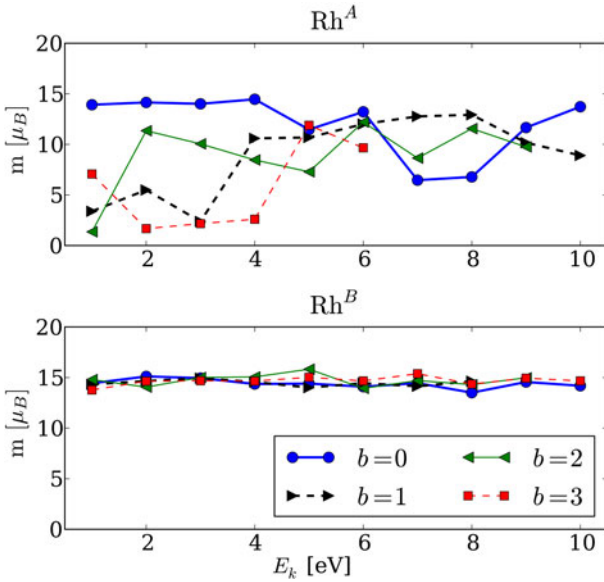


Fig. 7. (Color online) Average magnetic moment of the system, after the collision that leads to fusion of a Rh atom with Rh^A and Rh^B targets.

system as isolated. We did however investigate what happens when one keeps the spin fixed during the collision dynamics and observed that since the system is forced into a state that is not the ground state it is more likely to evolve into high symmetry excited state configurations.

The magnetic moment of Rh clusters was investigated by Kumar and Kawasoe [34] with emphasis on the symmetry of the system. They observed that icosahedral structures have much larger magnetic moments than the cubic ones, which underlies the strong relation between the geometrical structure and the magnitude of the magnetic moment. Thus, it seems pertinent to focus attention on the system magnetic configuration during the collision, as the cluster undergoes strong structural changes. We display in Figure 7 the average magnetic moment m during the collision, before the cooling process is initiated. It is quite apparent from the figure that m is strongly dependent on the target structure. The simplest behavior is the one illustrated in the lower panel, for the 13 atom system formed by the projectile atom plus Rh^B . The average magnetic moment is $\langle m \rangle \approx 15\mu_B$, for all b and E_k values. However, the magnitude of m during the dynamics is far from constant, rapidly oscillating between ~ 8 and $\sim 20\mu_B$. This is a consequence of the fact that the elastic energies are so much larger than the magnetic ones, and therefore the spin of the system is forced to quickly adapt to the cluster geometry. On the contrary, if the spin is kept fixed the opposite occurs: it is the spin that dominates the dynamics, with the geometry evolving very rapidly.

The evolution of the magnetization of the system, projectile atom plus Rh^A , is quite different from the simple average for the Rh^B target. The magnetization m varies markedly as a function of projectile energy, except for the $b = 0$ and projectile energy $E_k < 4$ eV case, where the variation of m is quite small. The explanation of this fea-

ture is the same we outlined above when studying the average temperature, namely, that for $b = 0$ the dynamics is like a typical molecular dynamics, while for $b \neq 0$ a large part of the collision dynamics is governed by the rearrangement of blocks of atoms.

Figure 5 displays the time dependence of the potential energy V with and without spin-polarization. The impact occurs at the first deep minimum of the V vs. t plot. During the early stages after impact both curves exhibit the same features, in spite of the lower energy of the spin-polarized cluster, which indicates that the same atomic rearrangement occurs regardless of the spin-polarization, i.e., the dynamics is projectile-driven. At ≈ 400 fs of simulation time the two curves fork out. The projectile has already delivered its kinetic energy and the energetics of the system is now driven by the bond dynamics and their rearrangements and, as already remarked, the bonds are stronger when spin-polarization is included. This behavior is quite independent of the target configuration, the magnitude of the impact parameter b and the kinetic energy E_k . The projectile-driven regime can last between 300 and 600 fs.

The changes in the electron level structure when allowing for spin polarization are very strong, since the levels display fast and wide oscillations, in contrast to the non-polarized treatment which exhibits just small oscillations. This difference is observed during the entire collision simulation, even during its early stages ($t < 0.3$ –0.4 ps), which is due to the fact that the variations of majority and minority spin occupation only generate energy variations of the order of 0.1 eV, much smaller than the changes due to ionic motion. An additional feature of Rh clusters is that, even for minor ionic rearrangements, it is likely that energy levels cross the Fermi level, with the cluster changing from conductor to half-metal and to semiconductor.

5 Summary and conclusions

In summary, we have investigated, by means of DFT molecular dynamics, the collision of a single Rh atom with two different 12 atom Rh configurations (a low energy and a compact one). The main variables that determine the dynamics of the process are the impact parameter b , and the kinetic energy E_k . However, the relation between magnetic and geometric configuration is far from simple.

We find that, in contrast with similar full d -shell gold atom cluster collisions, fusion of projectile and cluster is by far the most likely result [6]. Depending on the b and E_k values a rich variety of configurations is generated by the collisions, after which the fusion of projectile and target is the dominant outcome, with some modifications of the geometrical configurations due to spin polarization. Actually, when spin polarization is included it inhibits fragmentation, at least in the energy range up to $E_k = 10$ eV we have investigated. The other possible outcome, scattering, occurs rarely and only when spin polarization is taken consideration.

It is also worthwhile to notice that the study of the collisions yields an extra bonus, namely the possibility

of generating a rich variety of low energy configurations. These structures constitute an excellent data bank [33] in the search for the ground state energy configuration. As the cluster wanders around phase space, during its high temperature dynamics, it visits the basin of many different low energy configurations. Hence, we may be able to use these low energy configurations, corresponding to the minima of the V vs. t plot, as seeds that can be subsequently relaxed by DFT to low energy minima, yielding good candidates for ground state structures. This procedure bears some similarity with the work of Sun et al. [15,16], who combined a descriptor space global optimization method (taboo search) with energy evaluations. In essence, they applied high temperature DFT dynamics to an arbitrary structure and quenched promising low energy configurations in the search for putative minima. Of particular interest is the highly asymmetric lowest energy Rh_{13} configuration found so far [15,16], which corresponds to the $\{E_k = 1, b = 1, 2, 3\}$ of the spin polarized, and $\{E_k = 1, b = 0\}$ of the spin unpolarized structures illustrated in Figure 2.

Both our procedure, and the one due to Sun et al. [15,16], incorporate high temperature DFT dynamics to create promising minimal energy configurations, which are difficult to reach otherwise. This is due to the enormous number of local minima in phase space which are far from the main attractor and are very unlikely to be reached using high temperature molecular dynamics, which operates in a quasi-ergodic way exploring just a limited region of phase space due to computational time constraints. Thus, many relevant configurations are ignored by molecular dynamics during the energy minimization process. Nevertheless, it is important to keep in mind that our high temperature DFT dynamics is target dependent. This might constitute a drawback but it does give our method an additional degree of freedom, namely, the choice of the target structure.

In conclusion, to insure an adequate description of the collision dynamics of Rh clusters it is necessary to implement a spin-polarized treatment, since the magnetic configuration considerably alters the electronic structure. We expect a similar behavior for the other partially filled *d*-shell metals.

References

- N. Andersen, J.W. Gallagher, I.V. Hertel, Phys. Rep. **278**, 165 (1988)
- N. Andersen, J.T. Broad, E.E.B. Campbell, J.W. Gallagher, I.V. Hertel, Phys. Rep. **278**, 107 (1997)
- N. Andersen, K. Bartschat, J.T. Broad, I.V. Hertel, Phys. Rep. **279**, 251 (1997)
- C.H. Chien, E. Blaisten-Barojas, M.R. Pederson, J. Chem. Phys. **112**, 2301 (2000)
- J. Rogan, R. Ramírez, A.H. Romero, M. Kiwi, Eur. Phys. J. D **28**, 219 (2004)
- F. Muñoz, J. Rogan, G. García, M. Ramírez, J. Valdivia, R. Ramírez, M. Kiwi, Eur. Phys. J. D **61**, 87 (2011)
- A.J. Cox, J.G. Louderback, L.A. Bloomfield, Phys. Rev. Lett. **71**, 923 (1993)
- A.J. Cox, J.G. Louderback, S.E. Apsel, L.A. Bloomfield, Phys. Rev. B **49**, 12295 (1994)
- G. Schmid, *Nanoparticles: from theory to application* (Wiley-VCH, 2004), ISBN 3527305076
- J. Wei, E. Iglesia, J. Catal. **225**, 116 (2004)
- P. Nolte, A. Stierle, N.Y. Jin-Phillipp, N. Kasper, T.U. Schulli, H. Dosch, Science **321**, 1654 (2008)
- Y.C. Bae, V. Kumar, H. Osanai, Y. Kawazoe, Phys. Rev. B **72**, 125427 (2005)
- L. Wang, D. Johnson, Phys. Rev. B **75**, 235405 (2007)
- M.J. Piotrowski, P. Piquini, J.L.F. Da Silva, Phys. Rev. B **81**, 155446 (2010)
- Y. Sun, M. Zhang, R. Fournier, Phys. Rev. B **77**, 075435 (2008)
- Y. Sun, R. Fournier, M. Zhang, Phys. Rev. A **79**, 043202 (2009)
- Y. Jinlong, F. Toigo, W. Kelin, Z. Manhong, Phys. Rev. B **50**, 7173 (1994)
- P. Hohenberg, W. Kohn, Phys. Rev. B **136**, 834 (1964)
- W. Kohn, L.J. Sham, Phys. Rev. A **140**, 1133 (1965)
- G. Kresse, J. Hafner, Phys. Rev. B **47**, 558 (1993)
- G. Kresse, J. Furthmüller, Comput. Mater. Sci. **6**, 15 (1996)
- G. Kresse, J. Furthmüller, Phys. Rev. B **54**, 11169 (1996)
- G. Kresse, D. Joubert, Phys. Rev. B **59**, 1758 (1999)
- J.P. Perdew, K. Burke, M. Ernzerhof, Phys. Rev. Lett. **77**, 3865 (1996)
- J.P. Perdew, A. Zunger, Phys. Rev. B **23**, 5048 (1981)
- J.P. Perdew, Y. Wang, Phys. Rev. B **45**, 13244 (1992)
- F. Aguilera-Granja, J.L. Rodríguez-López, K. Michaelian, E.O. Berlanga-Ramírez, A. Vega, Phys. Rev. B **66**, 224410 (2002)
- F. Aguilera-Granja, J. Montejano-Carrizalez, R. Guirado-López, Phys. Rev. B **73**, 115422 (2006)
- Y.C. Bae, H. Osanai, V. Kumar, Y. Kawazoe, Phys. Rev. B **70**, 195413 (2004)
- C. Chang, M. Chou, Phys. Rev. Lett. **93**, 133401 (2004)
- T. Futschek, M. Marsman, J. Hafner, J. Phys.: Condens. Matter **17**, 5927 (2005)
- B.V. Reddy, S.K. Nayak, S.N. Khanna, B.K. Rao, P. Jena, Phys. Rev. B **59**, 5214 (1999)
- J. Rogan, M. Ramírez, V. Muñoz, J.A. Valdivia, G. García, R. Ramírez, M. Kiwi, J. Phys.: Condens. Matter **21**, 084209 (2009)
- V. Kumar, Y. Kawazoe, Eur. Phys. J. D **24**, 2301 (2003)
- M. Kalweit, D. Drikakis, Phys. Rev. B **74**, 235415 (2006)
- M.M. Mariscal, S.A. Dassie, E.P.M. Leiva, J. Chem. Phys. **123**, 184505 (2005)
- D. Alamanova, V.G. Grigoryan, M. Springborg, J. Phys. Condens. Matter **19**, 346204 (2007)